

Final Report

Title: A numerical study of vortex dynamics of flexible wing propulsors

AFOSR/AOARD Reference Number: AOARD-09-4077
AFOSR/AOARD Program Manager: Lt.Col. John Seo

Period of Performance: September 2009 - December 2010

Submission Date: March 30, 2011

Kartik Venkatraman
Associate Professor
Department of Aerospace Engineering
Indian Institute of Science
Bangalore 560012, India

Report Documentation Page			<i>Form Approved OMB No. 0704-0188</i>		
<p>Public reporting burden for the collection of information is estimated to average 1 hour per response, including the time for reviewing instructions, searching existing data sources, gathering and maintaining the data needed, and completing and reviewing the collection of information. Send comments regarding this burden estimate or any other aspect of this collection of information, including suggestions for reducing this burden, to Washington Headquarters Services, Directorate for Information Operations and Reports, 1215 Jefferson Davis Highway, Suite 1204, Arlington VA 22202-4302. Respondents should be aware that notwithstanding any other provision of law, no person shall be subject to a penalty for failing to comply with a collection of information if it does not display a currently valid OMB control number.</p>					
1. REPORT DATE 31 MAR 2011	2. REPORT TYPE Final	3. DATES COVERED 01-08-2009 to 28-02-2011			
4. TITLE AND SUBTITLE A numerical study of vortex formation and shedding from flapping flexible wing propulsors			5a. CONTRACT NUMBER FA23860914077		
			5b. GRANT NUMBER		
6. AUTHOR(S) Kartik Venkatraman			5c. PROGRAM ELEMENT NUMBER		
			5d. PROJECT NUMBER		
			5e. TASK NUMBER		
7. PERFORMING ORGANIZATION NAME(S) AND ADDRESS(ES) Indian Institute of Science, AE 606, Department of Aerospace Engineering, Bangalore 560012, India, NA, NA			5f. WORK UNIT NUMBER		
			8. PERFORMING ORGANIZATION REPORT NUMBER N/A		
9. SPONSORING/MONITORING AGENCY NAME(S) AND ADDRESS(ES) AOARD, UNIT 45002, APO, AP, 96338-5002			10. SPONSOR/MONITOR'S ACRONYM(S) AOARD		
			11. SPONSOR/MONITOR'S REPORT NUMBER(S) AOARD-094077		
12. DISTRIBUTION/AVAILABILITY STATEMENT Approved for public release; distribution unlimited					
13. SUPPLEMENTARY NOTES					
14. ABSTRACT <p>An airfoil or a wing-section oscillating in a fluid flow models the locomotion of certain aquatic and avian animals that propel themselves by flapping their fins and wings. The wing or the wing-section is usually flexible. It is well known that modeling the deformation in the flexible structure as a traveling wave, certain kinds of wave motion lead to high values of thrust and propulsive efficiency in a fluid. These results point to how some animals achieve high efficiencies during locomotion. However, these investigations do not account for the dynamics of the flexible structure interacting with the unsteady fluid dynamics. Here, a numerical simulation coupling the fluid and structure dynamics shows that high propulsive efficiencies are a consequence of fluid-elastic interaction and not some prescribed motions of the solid structure in a moving fluid.</p>					
15. SUBJECT TERMS Vortex flows, bio-inspired flights, Fluid Dynamics					
16. SECURITY CLASSIFICATION OF:			17. LIMITATION OF ABSTRACT Same as Report (SAR)	18. NUMBER OF PAGES 13	19a. NAME OF RESPONSIBLE PERSON
a. REPORT unclassified	b. ABSTRACT unclassified	c. THIS PAGE unclassified			

Abstract

An airfoil or a wing-section oscillating in a fluid flow models the locomotion of certain aquatic and avian animals that propel themselves by flapping their fins and wings. The wing or the wing-section is usually flexible. It is well known that modeling the deformation in the flexible structure as a traveling wave, certain kinds of wave motion lead to high values of thrust and propulsive efficiency in a fluid. These results point to how some animals achieve high efficiencies during locomotion. However, these investigations do not account for the dynamics of the flexible structure interacting with the unsteady fluid dynamics. Here, a numerical simulation coupling the fluid and structure dynamics shows that high propulsive efficiencies are a consequence of fluid-elastic interaction and not some prescribed motions of the solid structure in a moving fluid.

1 Introduction

The study of the fluid-elastic interaction of an oscillating flexible foil models locomotion in aquatic and avian animals, physiological phenomena such as snoring and coughing, and also the flapping of flags and filaments. The deforming solid is a moving boundary to the fluid dynamics model, and on the other hand, the fluid flow over the solid is equivalent to a distributed forcing or excitation to the dynamics of the deforming solid. Choice of appropriate models and accurate solution of the fluid-elastic equations are critical to simulating and understanding the phenomenon.

Oscillating rigid airfoils and the unsteady forces on them have been analyzed using different flow models. Plunge or heave motion, that is vertical transverse oscillation, of a rigid thin airfoil, is known to generate net thrust over a cycle of oscillation. Analysis carried out by [Garrick \(1937\)](#) using Theodorsen's unsteady potential flow theory shows that the propulsive efficiency of a harmonically plunging airfoil decreases with increase in the frequency of the plunging motion. A rigid airfoil not only can plunge or heave, but also perform angular oscillations about a pivot - also known as pitching motion. [Jones & Platzer \(1997\)](#) using a discrete vortex model of the unsteady potential flow, analyzed sinusoidal pure heave and pitch oscillations, as well as combined heave-pitch motions. With respect to sinusoidal plunge motion, they report that the propulsive efficiency indeed decreases with increase in the frequency of oscillation of the flat plate, whereas the thrust coefficient increases with increase in frequency of oscillation in plunge. In other words, at low frequencies of oscillation, very little thrust is generated very efficiently, and at high frequencies, very high thrust is generated albeit inefficiently. These results agree qualitatively and quantitatively with those of Garrick's result.

The two references cited above deal with a rigid flat plate oscillating in a potential flow. They provide a baseline for comparing our results as a consequence of fluid-elastic interactions. However, in the phenomenon that we are interested, the wing or wing-section is usually flexible, both chord-wise and span-wise. Limiting the circumference of our inquiry to chord-wise flexibility or a one-dimensional elastic solid structures in a two-dimensional potential flow, we review few highlights in the existing literature.

[Lighthill \(1960\)](#) usually is the starting point in any review on flapping propulsors. Although not exactly a true fluid-elastic model, the time-varying deformation of the structure is represented as a traveling transverse wave, and the thrust and propulsive efficiency computed from analysis of a moving boundary perturbing a three-dimensional potential flow - a typical slender body flow analysis. Lighthill showed that traveling waves of certain speed and shape lead to high values of thrust and propulsive efficiency. In particular, deformations of a slender body in a potential fluid flow that generate thrust at high efficiencies are traveling wave-like undulations whose phase speed is $5/4^{\text{th}}$ the free-stream speed. Further, these time-varying deformations that generate thrust at high efficiencies have positive and negative slopes to minimize recoil, and the slope at the tip is close to zero. These results agree well with observations made on a certain class of aquatic animal propulsors.

One of the first studies on the effect of fluid-elastic interaction was by [Katz & Weihs \(1978a\)](#) using an unsteady potential flow model about a flexible foil. The foil is assumed to be fixed at its leading edge and the flexibility effects

are included by allowing the cantilever beam to deform statically under the fluid dynamic forces. The conclusion of their study was flexibility increases the propulsive efficiency by 20% while causing a marginal decrease in thrust coefficient.

More recently, Prempraneerach *et al.* (2003) performed experiments in a water tunnel on a NACA 0014 airfoil made of flexible urethane foam undergoing combined heave-pitch oscillations. They characterized the flexibility of the airfoil in terms of its static stiffness. Two important findings of their investigations was that one, the thrust coefficient does not change appreciably with change in the stiffness of the airfoil, and two, the propulsive efficiency the flexible flapping airfoil increases by 36% relative to a rigid flapping foil.

Pederzani & Haj-Hariri (2006a) numerically analysed a heaving flexible airfoil in a two-dimensional viscous flow. Their results show that heavier airfoils are more efficient then lighter ones in generating thrust. However, this high efficiency is at the cost of low output thrust power or essentially low value of thrust over one cycle.

We now turn our attention to the flutter of filaments and flags. We know that flutter is a fluid-elastic dynamic instability. Since our interest is in thrust generated by a forced oscillation of a flexible foil in a fluid, we would like to know the regions in the parameter space where instabilities occur. This would, in turn, point to regions of resonance of the fluid-elastic system. Resonance of a system is also the state when the admittance or receptance of a system to external excitation is very high. This should in effect lead to high efficiencies. It is of interest to study whether this is indeed the case, and if so what is the variation of thrust and the nature of the wake vortex structure shed from the flexible foil.

The stability of a one-dimensional filament in a two-dimensional fluid has been the subject of interest in understanding the flapping of flags and filaments in a fluid flow. Zhang *et al.* (2000) examined the stability of a filament in a flow using a flowing soap film experiment. They observed that the length of the filament was a critical parameter in that below a critical length the filament's stretched straight configuration was the stable state to which any perturbations of the film returned. Above the critical length, there existed two stable states - one, the stretched straight state and a second flapping state with a finite amplitude. Hysteresis existed in passing from one stable state to the other. The vortex wake behind the stretched straight state was similar to a Bénard-Kármán vortex street, whereas the flapping state shed a wake akin to that observed in a Kelvin-Helmholtz instability. In the flapping state they observed that the trailing-edge amplitude showed variations with change in filament length though the frequency of flapping was almost constant.

Fitt & Pope (2001) showed the dependence of flutter instability of a filament in a two-dimensional potential flow on the mass ratio - roughly the ratio of fluid density to the density of the solid - and the flexural rigidity of the elastic filament. In particular, for a very rigid foil, the fluid-elastic system is stable for the entire mass ratio range. However, at low flexural rigidity values, flutter is a possibility at low mass ratios. This conclusion holds true for both hinged and clamped filaments.

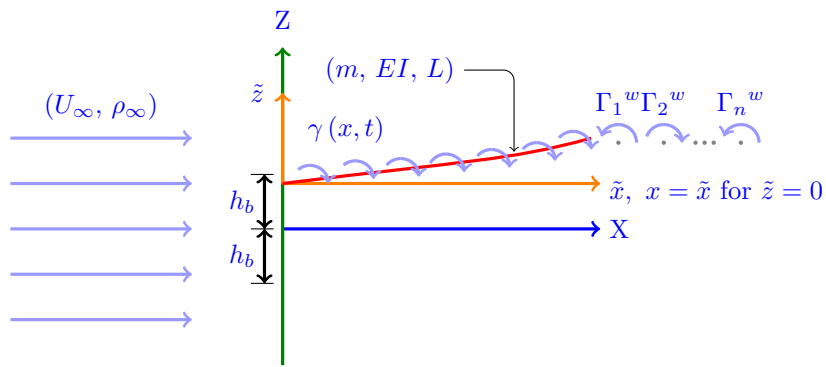
for of the fluid to thFitt & Pope (2001); Zhang *et al.* (2000); ?); Alben & Shelley (2008). These studies have implications to flapping wing locomotion in that regions of instability of a filament in a fluid flow could result in high

propulsive efficiencies. We will, on occasion, refer to some of these results to interpret our own

The work done in the past points to the fact that for a thin oscillating body in a fluid fluid-elastic interactions are important especially in relation to the propulsive forces that they generate. We explore this problem comprehensively. The present work includes the flexible body dynamics in computing the unsteady fluid forces as well as the inertial loading due to prescribed motion of the foil. The thrust coefficient and the propulsive efficiency are characterised in terms of a structural dynamic stiffness parameter and the mass ratio of the density of the foil material relative to that of the fluid. The structural dynamics is modeled as a cantilever Euler-Bernoulli beam with the leading edge fixed. The fluid flow over the foil is modeled as an unsteady two dimensional incompressible potential flow using discrete vortex elements. The equations of motion of the fluid and the structure are numerically integrated. A predictor-corrector algorithm couples the fluid-structure interaction. We compute the lift, the thrust, the wake vorticity, and the propulsive efficiency. The conclusions are that flexible and lighter foils generate more thrust more efficiently than a corresponding rigid foil. More significantly, the computed instantaneous deflected shape of the oscillating foil arrived at by coupling its fluid-elastic dynamics, closely correlate with the prescribed traveling wave motion in the beam as shown by [Lighthill \(1960\)](#). These results presented here point to the fact that efficient locomotion in animals often is a consequence of fluid-elastic interactions.

2 Fluid-structure interaction model

The fluid part is modeled using inviscid airfoil theory as well as incompressible viscous flow. The results for fluid structure interaction is presented in this document uses the inviscid airfoil theory for modeling fluid.



Consider a thin foil flapping in a inviscid flow, whose amplitude of oscillation is more than its length L . Initially the airfoil is at the origin of the inertial coordinate system X, Z denote the inertial coordinate system or the laboratory frame of reference and x, z denotes the foil coordinate system as shown in the figure below. The governing equation for the unsteady incompressible potential flow in the $\tilde{x} - \tilde{z}$ plane using thin airfoil theory [Katz & Plotkin \(2001\)](#) is given by

$$\nabla^2 \Phi = 0, \quad (1)$$

The disturbance potential Φ is modeled using the discrete vortex element which inherently satisfies the Kutta condition. The wake is modeled as a distributed set of vortices on a deforming sheet. The boundary conditions for equation 1 are that there is no flow through the plate surface $Z = h(X, t)$ and the disturbance decays far from the plate. The instantaneous strength of the vortex sheet leaving the beam's trailing edge can be calculated by Kelvin's theorem. The fluid dynamic pressures and loads generated by the foil is calculated using unsteady Bernoulli equation.

A finite element model of foil wing has been constructed, which incorporates the flexibility and mass properties into the structural model. The foil is assumed as a cantilever beam which is fixed at its leading edge. The equation of motion of beam that governs the transverse deformation due to the forces acting on it is

$$m \frac{\partial^2 \eta}{\partial t^2} + \frac{\partial^2}{\partial \zeta^2} \left[EI \frac{\partial^2 \eta}{\partial \zeta^2} + a_1 \frac{\partial^3 \eta}{\partial^2 \zeta \partial t} \right] = F_f(t) + F_i(t), \quad (2)$$

where η , EI , m , F_f , F_i are the transverse beam deflection, flexural rigidity, mass per unit length, unsteady hydrodynamic force per unit length, inertial force per unit length respectively. The constant a_1 is the stiffness proportionality factor (see [Clough & Penzein, 1993](#)). The non-dimensional form of the above equation is

$$\bar{\omega}_c^2 \frac{\partial^4 \bar{\eta}}{\partial \bar{x}^4} + \bar{a}_1 \bar{\omega}_c^2 \frac{\partial^5 \bar{\eta}}{\partial \bar{x}^4 \partial \tau} + \frac{\partial^2 \bar{\eta}}{\partial \tau^2} = \mu \left(\bar{\Gamma} + \int_0^1 \frac{\partial}{\partial \tau} \bar{\Gamma} d\zeta \right) - \frac{\partial^2 \bar{h}}{\partial \tau^2}. \quad (3)$$

The structural response of the cantilever beam model is defined in orthogonal system coordinate system with abscissa along the instantaneous undeflected foil direction. The finite element modeling is done by using the 2D beam element, which uses the Euler-Bernoulli beam theory. Structural response is evaluated by direct integration which uses Newmark's linear acceleration method (see [Cook *et al.*, 2002](#)). The unsteady fluid force due to fluid-structure interaction is obtained from the solution of potential flow field. Fully implicit coupling (see [Pederzani & Haj-Hariri, 2006b](#); [Bharadwaj *et al.*, 1998](#); [Katz & Weihs, 1978b](#)) is used for the fluid structure interaction of the flexible airfoil.

3 Results and Discussions

Inertial and elastic effects are studied on the foil exhibiting heaving motion. The foil is fixed at its leading edge and it moves with velocity U parallel to its length in undeformed state. The thrust coefficient of the foil is

$$C_T = \frac{2}{\rho c U^2} \frac{1}{T} \int_0^T \left(\sum F_x \cos \theta - \sum F_z \sin \theta \right) dt. \quad (4)$$

non-dimensional parameter	expression
$\bar{\omega}_c$	$\sqrt{\frac{EI}{mL^4}} \frac{L}{U}$
$\bar{\eta}$	$\frac{n}{L}$
$\bar{\zeta}$	$\frac{\zeta}{L}$
\bar{F}	$\frac{FL}{mU^2}$
\bar{a}_1	$\frac{a_1 L}{U}$
τ	$\frac{U}{L} t$
μ	$\frac{\rho L^2}{m}$
$\bar{\Gamma}$	$\frac{\Gamma}{LU}$

The propulsive efficiency, defined as the ratio of output power to input power, is given by

$$\eta_p = \frac{\frac{1}{T} \int_0^T \left(\sum F_x \cos \theta - \sum F_z \sin \theta \right) \frac{dS_x}{dt} dt}{\frac{1}{T} \int_0^T \left(\sum F_x \sin \theta - \sum F_z \cos \theta \right) \frac{dh}{dt} dt + \int_0^T M_y \frac{d\theta}{dt} dt}. \quad (5)$$

Forces F_x , F_z are the instantaneous forces along the x , z directions respectively. Moment M_y is the moment about axis y due to forces acting on the foil. The non-dimensional parameters mass ratio μ , characteristic frequency $\bar{\omega}_c$ are used to characterize the propulsive performance of the flexible foil.

An airfoil in heaving motion is known to produce thrust for all frequencies of heaving whereas airfoil in pitching will produce thrust above a certain threshold frequency of oscillation (see [Garrick, 1936](#)). Characteristic frequency $\omega_c \frac{L}{U}$ represents the flexibility parameter. Higher the value of characteristic frequency the foil is rigid and for lower values of characteristic frequency the foil is flexible. Figure 1(a) shows the variation of the thrust coefficient with respect to $\frac{\omega_c L}{U}$ for heaving case. The variation of thrust coefficient is shown for different values of $\frac{\Omega L}{U}$. As $\frac{\omega_c L}{U}$ decreases, the thrust coefficient increases. At lower values of $\frac{\omega_c L}{U}$, the foil deforms due to the fluid pressure acting on it. The deformed foil produces a force component along the forward velocity direction as shown in the Figure ???. Thus higher thrust coefficient is achieved for lower $\frac{\omega_c L}{U}$.

Figure 1(b) shows the variation of efficiency with respect to $\frac{\omega_c L}{U}$. As $\frac{\omega_c L}{U}$ reduces, more thrust is produced at the cost of decreased input effort. Thus higher efficiencies are achieved for lower values of $\frac{\omega_c L}{U}$. For higher frequency of heaving, the efficiency is low compared to lower frequency of heaving at larger

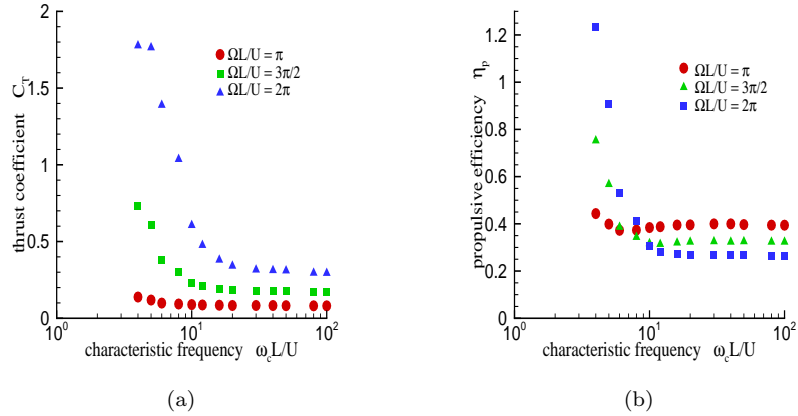


Figure 1: Effect of $\omega_c L/U$ on propulsive parameters, $\frac{H}{L} = 0.1$, $a_1 L/U = 0.000586$, $\mu = 10$.

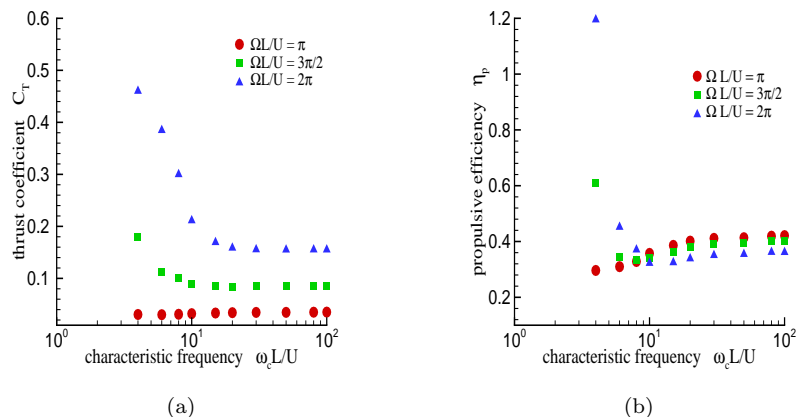


Figure 2: Effect of $\omega_c L/U$ on propulsive parameters, $\alpha_0 = 5^\circ$, $a_1 L/U = 0.000586$, $\mu = 10$.

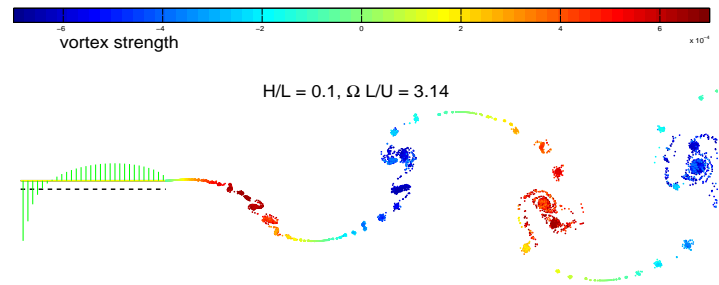


Figure 3: Wake patterns after three cycles of heaving rigid foil.

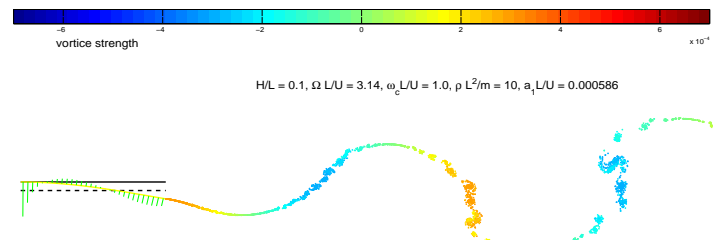


Figure 4: Wake patterns after three cycles of heaving flexible foil.

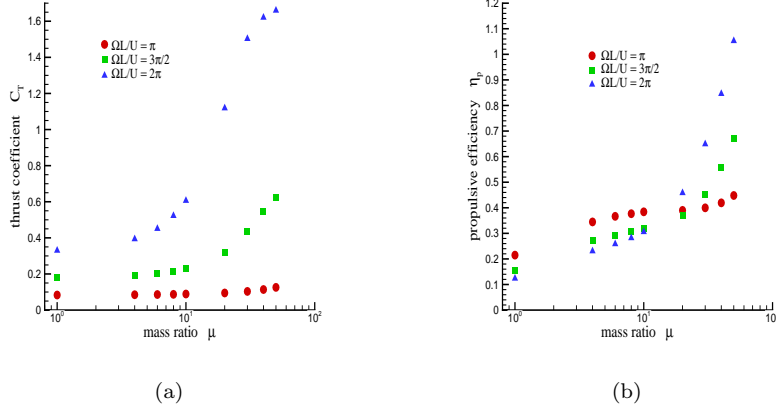


Figure 5: Effect of μ on propulsive parameters, $\frac{H}{L} = 0.1$, $a_1 L/U = 0.000586$, $\omega_c L/U = 10$.

values of ω_c , even though the thrust coefficient is high. This is due to the fact that more effort is spent in high frequency heaving for little improvement in thrust. But as the value of ω_c decreases, the higher pressure produces more thrust effect due to deformation of the foil. Thus the efficiencies are more for high frequency heaving at lower values of ω_c . Figure 2 shows the effect of characteristic frequency on the propulsive performance for pitching case. Similar explanation as that of heaving case holds good for the results shown in Figure 2.

Figure 3 shows the wake patterns at the end of three cycles of heaving motion for a rigid airfoil. Figure 4 shows the wake patterns at the end of three cycles of heaving motion with $\bar{\omega}_c = 1$. Clearly we can see the reverse Karman vortex street characterizing thrust producing system. For flexible foil, the strength of the vortex strength in the wake is less compared to the rigid case. And also the vortex roll up is not significant for the flexible foil.

Figure ?? shows the variation of thrust coefficient with respect to mass ratio for different plunging frequencies. Figure ?? shows the variation of propulsive efficiency with respect to mass ratio for different plunging frequencies. Larger the mass ratio, greater the fluid forces causing the foil to bend. Thus greater propulsive performance is observed for larger values of mass ratio. Figure 6 shows effect of mass ratio on propulsive parameters for pitching motion. Similar explanation as that of heaving holds good for pitching also.

4 Concluding remarks

A combination of mass ratios and dynamic stiffness together with the excitation frequency and flow speed determines high efficiency and high thrust. In fact it may not be possible to achieve high thrust with high propulsive efficiency simultaneously.

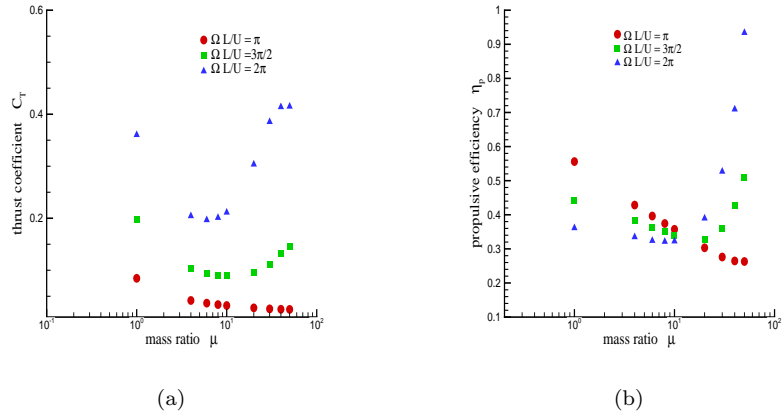


Figure 6: Effect of μ on propulsive parameters, $\alpha_0 = 5^\circ$, $a_1 L/U = 0.000586$, $\omega_c L/U = 10$.

5 Acknowledgement

The work presented in this thesis was carried out by Mysa Ravi Chaithanya, a doctoral candidate under the supervision of the author of this report.

References

ALBEN, SILAS & SHELLEY, MICHAEL J. 2008 Flapping states of a flag in an inviscid fluid: Bistability and the transition to chaos. *Physical Review Letters* **100** (7), 074301.

BHARADWAJ, M. K., RAKESH, K. & GURUSWAMY, G. P. 1998 A cfd/csd interaction methodology for aircraft wings. In *Symposium on Multidisciplinary Analysis and Optimization*. AIAA, St. Louis, MO.

CLOUGH, R. W. & PENZEN, J. 1993 *Dynamics of Structures*. McGraw-Hill, Inc.

COOK, R. D., MALKUS, D. S., PLESHA, M. E. & WITT, R. J. 2002 *Concepts and Applications of Finite Element Analysis*. Pearson.

FITT, A. D. & POPE, M. P. 2001 The unsteady motion of two-dimensional flags with bending stiffness. *Journal of Engineering Mathematics* **40**, 227–248.

GARRICK, I. E. 1936 Propulsion of a flapping and oscillating airfoil. *NACA Report* **567**.

GARRICK, I. E. 1937 Propulsion of a flapping and oscillating airfoil. *Tech. Rep. NACA-TR-567*. National Advisory Committee on Aeronautics.

JONES, K. D. & PLATZER, M. F. 1997 Numerical computation of flapping wing propulsion and power extraction. AIAA 35th Aerospace Sciences Meeting & Exhibit, Reno, NV, USA.

KATZ, J. & PLOTKIN, A. 2001 *Low Speed Aerodynamics*. Cambridge University Press.

KATZ, J. & WEIHS, D. 1978a Hydrodynamic propulsion by large amplitude oscillation of an airfoil with chordwise flexibility. *Journal of Fluid Mechanics* **88**, 485–497.

KATZ, J. & WEIHS, D. 1978b Hydrodynamic propulsion by large amplitude oscillation of an airfoil with chordwise flexibility. *Journal of Fluid Mechanics* **88**, 485–497.

LIGHTHILL, M. J. 1960 Note on the swimming of slender fish. *Journal of Fluid Mechanics* **9**, 305–317.

PEDERZANI, J. & HAJ-HARIRI, H. 2006a Numerical analysis of heaving flexible foils in a viscous flow. *AIAA Journal* **88**, 2773–2779.

PEDERZANI, J. & HAJ-HARIRI, H. 2006b Numerical analysis of heaving flexible foils in a viscous flow. *AIAA Journal* **88**, 2773–2779.

PREMPRANEERACH, P., HOVER, F. S. & TRIANTAFYLLOU, M. S. 2003 The effect of chordwise flexibility on the thrust and efficiency of a flapping foil. In *Proceedings of the 13th International Symposium on Unmanned Untethered Submersible Technology*. Autonomous Undersea Systems Institute, Durham, New Hampshire.

ZHANG, J., CHILDRESS, S., LIBCHABER, A. & SHELLEY, M. 2000 Flexible filaments in a flowing soap film as a model for one-dimensional flags in a two-dimensional wind. *Nature* **408**, 835–839.